

# Sb-surfactant-mediated growth of Si/Si<sub>1-y</sub>C<sub>y</sub> superlattices by molecular-beam epitaxy

P. O. Pettersson, C. C. Ahn, and T. C. McGill<sup>a)</sup>

Department of Applied Physics, California Institute of Technology, Pasadena, California 91125

E. T. Croke and A. T. Hunter

Hughes Research Laboratories, Malibu, California 90265

(Received 22 June 1995; accepted for publication 16 August 1995)

Si/Si<sub>0.97</sub>C<sub>0.03</sub> superlattices were grown on Si(001) substrates by molecular beam epitaxy (MBE) to study the use of Sb as a surfactant during Si<sub>1-y</sub>C<sub>y</sub> growth. *In situ* reflection high energy electron diffraction (RHEED) shows that while carbon easily disrupts the two-dimensional growth of homoepitaxial Si, such disruption is suppressed for layers grown on Sb-terminated Si(001) surfaces. Cross-sectional transmission electron microscopy (TEM) reveals that for samples grown without the use of Sb, the Si/Si<sub>0.97</sub>C<sub>0.03</sub> interfaces (Si<sub>0.97</sub>C<sub>0.03</sub> on Si) were much more abrupt than Si<sub>0.97</sub>C<sub>0.03</sub>/Si interfaces. In the case of Sb-mediated growth, differences in abruptness between the two types of interfaces were not readily observable. © 1995 American Institute of Physics.

The introduction of carbon into the Si/Ge material system offers the potential of increased flexibility in the design of strain and electronic structure in Si-based electronics. Due to the smaller lattice constant of diamond ( $a_0=0.357$  nm versus  $a_0=0.543$  nm for Si and  $a_0=0.566$  nm for Ge), carbon could be used for strain compensation of SiGe structures, resulting in alloy layers which are lattice matched to Si and therefore in devices that are stable during high temperature processing. In addition, the introduction of carbon may provide useful conduction band offsets for layers grown on Si, allowing the possibility for novel *n*-type devices such as *n*-type resonant tunneling devices (RTDs) or high-electron-mobility transistors (*n*-HEMTs) to be compatible with VLSI processing lines.

For Si<sub>1-x</sub>Ge<sub>x</sub> layers grown coherently strained to Si(001), Van de Walle and Martin<sup>1</sup> predict that the strain-induced splitting of the six-fold-degenerate conduction band lowers the four-fold-degenerate valley enough to compensate the slight increase in energy associated with the introduction of Ge. The net result is little or no conduction band offset (for  $x<0.5$ ). One way to overcome this problem has been to grow Si under tension on a relaxed Si<sub>1-x</sub>Ge<sub>x</sub> buffer layer.<sup>2</sup> The problem with this approach is typically that the relaxed Si<sub>1-x</sub>Ge<sub>x</sub> layer is defective and the processing possibilities are constrained.

The introduction of carbon into the Si<sub>1-x</sub>Ge<sub>x</sub>/Si material system could result in significant conduction band offsets, without the above problems. For example, carbon could be used to reduce the lattice constant of Si<sub>1-x</sub>Ge<sub>x</sub> and eliminate the strain-induced splitting of the bands. This effect could lead to a significant increase in the conduction band offset. However, estimates by Powell *et al.*<sup>3</sup> of the band gap changes associated with the introduction of C into tensile-strained Si<sub>0.97</sub>C<sub>0.03</sub> alloys, predict only moderate effects until carbon concentrations in excess of 1% are achieved. Hence, we expect that substantially more than 1% carbon will be

required to produce band offset shifts larger than  $kT$  at room temperature.

Our experiments show that for carbon concentrations in excess of 2%, the normal layer-by-layer growth on Si(001)<sup>4</sup> is disrupted, resulting in a rough surface. This roughness manifests itself in RHEED as “spottness” in the pattern, rather than the streaked, (2×1)+(1×2) pattern associated with growth on atomically smooth, two-domain-reconstructed Si(001) surfaces.

In this letter, we report a study of surfactant-mediated growth of Si/Si<sub>0.97</sub>C<sub>0.03</sub> superlattices using RHEED and TEM. Composition and layer thicknesses were confirmed using high resolution x-ray diffraction (HRXRD). We show that the surfactant reduces the tendency for the Si<sub>1-y</sub>C<sub>y</sub> surface to roughen during growth, allowing the growth of layers with even higher carbon concentrations. This technique has been used to suppress Stranski-Krastanov islanding during the growth of Si/Ge superlattices<sup>5</sup> and Ge<sub>1-y</sub>C<sub>y</sub> alloy layers<sup>6</sup> on Si substrates.

The samples consisted of two 15-period, 26.1 nm Si/4.4 nm Si<sub>0.97</sub>C<sub>0.03</sub> superlattices grown at 525 °C on 100 nm thick Si buffer layers on substrates prepared as in Ref. 7. After the deposition of the Si buffer layer, approximately one monolayer ( $6.8 \times 10^{14}$  atoms/cm<sup>3</sup>) of Sb was deposited on sample SL-Sb. Sample SL received no such Sb predeposition. The superlattices were then grown on each sample using growth rates of  $\sim 1.8$  Å/s and  $\sim 0.015$  Å/s for Si and C, respectively. Closed loop control of the carbon flux was obtained by monitoring the amplitude of amu 36 (C<sub>3</sub>) with a residual gas analyzer (RGA) and adjusting the power to the electron gun to maintain a predetermined signal. During superlattice growth, images of the RHEED patterns were captured<sup>8</sup> for later analysis. The TEM cross sections were prepared by mechanical polishing and ion milling; the micrographs were acquired at an acceleration voltage of 300 kV on a Philips EM430 electron microscope.

The RHEED pattern from both samples prior to growth of the Si buffer layer exhibited the usual (2×1)+(1×2) streaked pattern typical of a clean Si(001) surface. During

<sup>a)</sup>Electronic mail: tcm@ssdp.caltech.edu

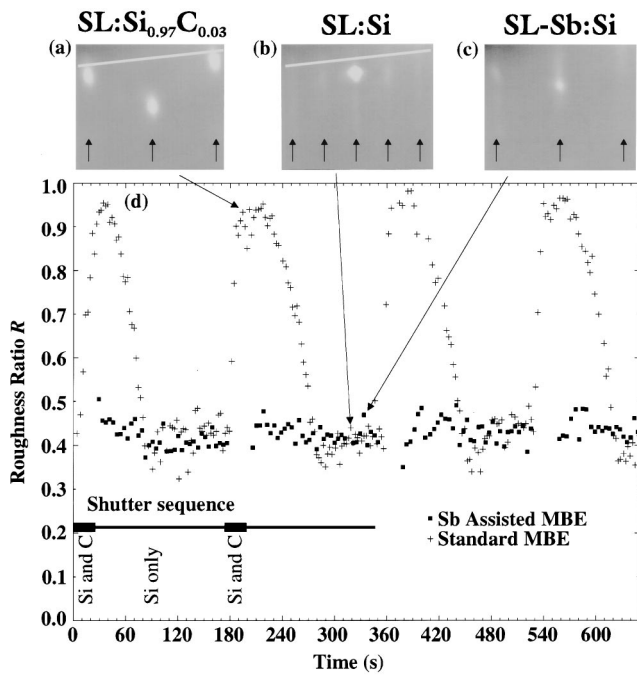


FIG. 1. Roughness ratio  $R$  versus growth time (d). An  $R$  of 1 indicates a spotted RHEED pattern and an  $R$  of 0.4 indicates a streaked pattern. The RHEED images shown in (a)–(c) were acquired at the point of the growth sequence indicated by the long arrows. The short arrows in (a)–(c) mark the positions of the streaks/spots.

growth of sample SL, immediately upon opening the carbon shutter, the pattern became spotty, indicative of a rough surface. Each subsequent Si layer caused the pattern to revert to the  $(2 \times 1)$ -reconstructed pattern, suggesting that the Si deposition caused the surface to become smooth again. This alternating behavior of roughening followed by smoothing persisted throughout the growth of this sample. For sample SL-Sb, the half-order streaks diminished in intensity after Sb deposition. The observed  $(1 \times 1)$  pattern remained streaked during the subsequent growth of the superlattice.

To differentiate between the spotted and streaked RHEED patterns (sample SL), we analyzed the data as follows. First, the intensity along a line [marked in white in Figs. 1(a) and 1(b)] perpendicular to the streak direction and intersecting the  $(10)$  and  $(\bar{1}0)$  spots was digitized. Then, the intensity associated with a certain spot or streak ( $n0$ ) was integrated along the line, to take into account the intensity from the full width of the streak or spot, to give the quantity  $I_{n0}$ . The background intensity due to light from the e-gun sources was subtracted. Finally, we calculated the ratio,  $R$ , of the spot intensity to the intensity of the whole pattern [see Eq. (1)]. This ratio can be used as a qualitative measure of surface roughness. For a spotty pattern,  $I_{\bar{1}0}$  and  $I_{10}$  will dominate, making  $R \approx 1$ . On the other hand, when the RHEED pattern is streaked [see Figs. 1(b)], all the terms are of comparable magnitude, giving an  $R$  of about  $\frac{2}{5} = 0.4$ ;

$$R = \frac{I_{\bar{1}0} + I_{10}}{I_{\bar{1}0} + I_{\frac{1}{2}0} + I_{00} + I_{\frac{1}{2}0} + I_{10}} \quad (1)$$

In Fig. 1(d), the ratio,  $R$ , is plotted as a function of time during growth of the two samples (C shutter opens at  $t = 0$  s).

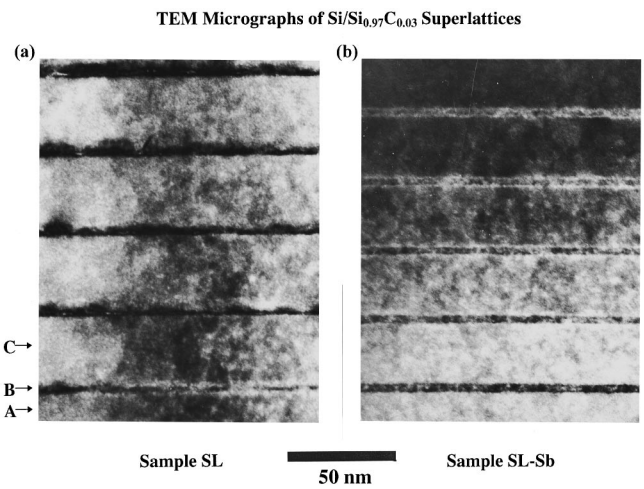


FIG. 2. Cross-sectional TEM images of the superlattice samples. (a) shows sample SL. The alternating layers of light (C) and dark (B) bands correspond to the Si and  $\text{Si}_{0.97}\text{C}_{0.03}$  layers, respectively. The Si buffer layer is marked A near the bottom of the figure. The interfaces which are formed when  $\text{Si}_{0.97}\text{C}_{0.03}$  is grown on Si are much more abrupt than the interfaces formed when Si is grown on  $\text{Si}_{0.97}\text{C}_{0.03}$ . In the case of sample SL-Sb (b), both interfaces appear equally abrupt.

The RHEED images shown in Figs. 1(a)–1(c) were acquired at the point in the growth sequence indicated by the arrows. For sample SL (no Sb predeposition), immediately upon opening the C shutter the ratio is shown to increase rapidly, saturating at a value near 1. During subsequent growth of the Si layer, the RHEED pattern slowly recovered its original  $(2 \times 1) + (1 \times 2)$ , streaked pattern and the ratio returned to approximately 0.4 (smooth). From Fig. 1(d), we note that fully half ( $\approx 13$  nm) of the Si layer thickness was required to completely recover the original pattern. During growth of sample SL-Sb, the RHEED pattern remained unchanged from the  $(1 \times 1)$ , streaked pattern was observed immediately following Sb predeposition. Data were not available for SL-Sb during  $\text{Si}_{0.97}\text{C}_{0.03}$  deposition because stray light from the e-guns washed out the pattern. Nevertheless, it was possible to view the pattern visually during these periods and no spottiness was observed.

In Fig. 2, we present cross-sectional TEM images of the samples which show features consistent with the RHEED observations. Figure 2(a) is an image taken from sample SL, showing alternating layers of light and dark bands corresponding to the Si and  $\text{Si}_{0.97}\text{C}_{0.03}$  layers, respectively. The  $\text{Si}_{0.97}\text{C}_{0.03}$  layers might appear thinner in Fig. 2(a) (sample SL) compared to the  $\text{Si}_{0.97}\text{C}_{0.03}$  layers in Fig. 2(b) (sample SL-Sb) due to the diffuse nature of the interfaces of sample SL. The Si buffer layer (marked A) is near the bottom of the figure. For sample SL, the interfaces which are formed when  $\text{Si}_{0.97}\text{C}_{0.03}$  is grown on Si are much more abrupt than the interfaces formed when Si is grown on  $\text{Si}_{0.97}\text{C}_{0.03}$ . For sample SL-Sb [Fig. 2(b)], both interfaces appear equally abrupt. In comparison with sample SL, they appear more abrupt than the case for which Si is grown on  $\text{Si}_{0.97}\text{C}_{0.03}$  and less abrupt than the case for which  $\text{Si}_{0.97}\text{C}_{0.03}$  is grown on Si.

Our observations suggest that one or more species in the carbon flux form surface nucleation centers where diffusing adatoms can incorporate in competition with surface steps,

resulting in 3D growth. In principle, any of the monomers (C), dimers ( $C_2$ ), and trimers ( $C_3$ ) present (as measured by RGA) in the growth flux could be responsible for the nucleation centers. Since the monomers have the highest mobility, they are the most likely ones to be incorporated in step-flow growth.

All of the multiple carbon species are potential candidates for nucleating the rough growth. First, since the C—C bond is 1.8 times stronger<sup>9</sup> than the Si—Si bond which is stable up to 600 K,<sup>10</sup> the C dimers and trimers should be stable up to 1100 K; since the growth temperature was 525 °C, the carbon dimers and trimers impinging on the surface should remain undissociated.

Second, because of the large activation energy due to the bond bending and stretching required for a dimer or trimer to move on the surface, the diffusion lengths of these species are expected to be negligible compared to that of the monomers. Thus, the dimers or trimers could be expected to incorporate at the site of impingement and form nucleation centers.

Third, the nucleation center density is large enough for 3D growth to dominate over 2D step flow growth. To show one possibility for how this could occur, we consider the probability of an adatom attaching to a dimer rather than to a step. To assess the relative probability, we follow the argument of Mo *et al.*<sup>10</sup> We consider a square with a dimer at the center and one side aligned with a step on a slightly miscut substrate. The length of the side is equal to the average terrace width  $W$  of the steps given by the degree of miscut. Under the conditions of our experiment, this square is the area from which this portion of the step accumulates adatoms. According to the 2D random walk theory, the number of hops required for an adatom impinging at a random site in the square to reach the dimer is about the same as the number of hops required for it to reach the step. In this case then, both island growth and step flow growth take place. For both sample SL and SL-Sb, the fluxes of the dimers and trimers were about 10% and 5% of the monomer flux respectively. These fluxes yield a dimer and trimer density of about  $10^{12}$  molecules/cm<sup>2</sup> in the time required to grow a monolayer of  $Si_{0.97}C_{0.03}$ . Taking the limiting case of a wafer miscut by 0.5°, the terrace width is  $W \approx 2 \times 10^{-6}$  cm so  $W^2 \approx 4 \times 10^{-12}$  cm<sup>2</sup>. At the density calculated above, we expect four dimers per square so 3D nucleation should compete effectively with 2D step-flow growth.

We speculate that in the case of sample SL-Sb, where the surface stays smooth throughout the growth, the surfactant prevents carbon from forming effective nucleation centers. The primary role of the Sb is to ride as a surface layer bury-

ing the carbon molecules. An impinging silicon adatom diffuses on the Sb layer until it exchanges with a surfactant atom and incorporates. Again, the carbon clusters do not diffuse on the surface, rather they are incorporated immediately by some exchange mechanism. Since contact between Si adatoms and the carbon clusters is reduced, the clusters no longer form effective nucleation centers and the growth stays relatively smooth as shown by the streaked RHEED pattern.

The TEM picture in Fig. 2 shows that the interface between the Si and  $Si_{0.97}C_{0.03}$  on the substrate side is slightly rougher on the sample grown with Sb than it is on sample grown without Sb. One possible explanation is that a perfectly ordered Sb terminated Si(001) surface was not achieved. The unordered surface could prompt the exchange to occur at sites other than steps thus creating a less abrupt growth front. A highly ordered Sb-terminated ( $2 \times 1$ )-reconstructed surface could be expected to aid in the formation of perfectly flat interfaces.

In summary, we studied the effect of adding Sb as a surfactant in the MBE growth of  $Si/Si_{0.97}C_{0.03}$  superlattices. Our analysis shows that epitaxial growth on the ( $2 \times 1$ ) Si(001) surface could be easily disrupted by carbon dimers and trimers nucleating rough growth. The Sb surface layer could prevent contact between the carbon dimers and the silicon adatoms, suppressing the roughening of the surface. Hence, the use of Sb as a surfactant during growth of high-carbon-content  $Si_{1-x-y}Ge_xC_y$  alloys results in sharper film interfaces and is useful for achieving carbon contents in excess of what would normally be possible for growth on bare Si(001).

This study was supported in part by ONR N00014-93-1-0710. We are grateful for Carol Garland's assistance in obtaining the TEM images.

- <sup>1</sup>C. G. Van de Walle and R. M. Martin, Phys. Rev. B **34**, 5621 (1986).
- <sup>2</sup>E. A. Fitzgerald, Y.-H. Xie, D. Monroe, P. J. Silverman, J. M. Kuo, A. R. Kortan, F. A. Theil, and B. E. Weir, J. Vac. Sci. Technol. B **10**, 1807 (1992).
- <sup>3</sup>A. R. Powell, K. Eberl, F. K. LeGoues, B. A. Ek, and S. S. Iyer, J. Vac. Sci. Technol. B **11**, 1064 (1993).
- <sup>4</sup>Y.-W. Mo, R. Kariotis, D. E. Savage, and M. G. Lagally, Surf. Sci. **219**, L551 (1989).
- <sup>5</sup>K. Fujita, S. Fukatsu, H. Taguchi, T. Igarashi, Y. Shiraki, and R. Ito, Mater. Res. Soc. Symp. Proc. **220**, 193 (1991).
- <sup>6</sup>H. J. Osten, E. Bugiel, and P. Zaumel, J. Cryst. Growth **142**, 322 (1994).
- <sup>7</sup>E. T. Croke, M. J. Harrell, M. E. Mierzwinski, and J. D. Plummer, Mater. Res. Soc. Symp. Proc. **281**, 415 (1993).
- <sup>8</sup>D. A. Collins, T. C. Fu, T. C. McGill, and D. H. Chow, J. Vac. Sci. Technol. B **10**, 1779 (1992).
- <sup>9</sup>L. Pauling, *General Chemistry* (Dover, New York, 1988).
- <sup>10</sup>Y.-W. Mo, J. Kleiner, M. B. Webb, and M. G. Lagally, Surf. Sci. **268**, 275 (1992).

*Published without author corrections*